Polymer Degradation and Stability 94 (2009) 1405–1410

Contents lists available at ScienceDirect

Polymer Degradation and Stability

journal homepage: www.elsevier.com/locate/polydegstab

Preparation and controlled degradation of oxidized sodium alginate hydrogel

Chunmei Gao, Mingzhu Liu*, Jun Chen, Xu Zhang

Department of Chemistry and State Key Laboratory of Applied Organic Chemistry, Lanzhou University, Lanzhou 730000, People's Republic of China

ARTICLE INFO

Article history:
Received 26 February 2009
Received in revised form
9 May 2009
Accepted 17 May 2009
Available online 27 May 2009

Keywords:
Oxidized sodium alginate
Hydrogel
Degradation
Swelling kinetics

ABSTRACT

Degradation is often a critical property of materials utilized in tissue engineering. Although alginate, a naturally derived polysaccharide, is an attractive material due to its biocompatibility and ability to form hydrogels, its slow and uncontrollable degradation can be an undesirable feature. In this study, the degradation behavior of hydrogel based on oxidized sodium alginate (OSA) crosslinked with Ca^{2+} was studied in phosphate buffer solution (PBS, pH = 7.4) and Tris-(hydroxymethyl) aminomethane–HCl (Tris–HCl, pH = 7.4) at 37 °C. The degradation behavior of OSA hydrogels with different degrees of oxidation was evaluated as a function of degradation time by monitoring the changes of molecular weight and weight loss. It was found that the degradation behavior relied heavily on the degree of oxidation and the surrounding medium. This result indicates that the degradation rates of OSA hydrogels can be controlled by changing the degree of oxidation.

1. Introduction

Hydrogels, i.e. polymeric three-dimensional networks able to swell in the presence of an aqueous medium, are extensively employed in biomedical and pharmaceutical field as soft contact lenses, wound dressing, drug delivery systems, biosensors and implantable devices in tissue engineering [1–6]. For biomedical applications, it is often required that the hydrogel can degrade under physiological conditions [7].

Alginate, a water-soluble linear polymer obtained from brown algae, is composed of (1-4)-β-D-mannuronic acid (M) and (1-4)-a-L-guluronic acid (G) units in the form of homopolymeric (MM- or GG-blocks) and heteropolymeric sequences (MG- or GM-blocks). Bearing in mind their gelling ability, stabilizing properties and high viscosity in aqueous solutions, alginates and their derivatives are widely used in the food, cosmetics and pharmaceutical industries [8,9]. Since alginate is not naturally enzymatically degraded in mammals, months can be passed before alginate hydrogels are completely removed from implantation sites [10]. The degradation kinetics of alginate hydrogels have been previously controlled by varying alginate molecular weight, chemical structure, and by covalent crosslinking. Ionically crosslinked, high molecular weight alginate hydrogels degrade in an uncontrollable and unpredictable manner following the dissolution of calcium into the surrounding medium [11]. Furthermore, the molecular weight of intact alginate is typically above the renal clearance threshold, thus preventing it from being excreted from the body [12]. One previously reported approach to control alginate hydrogel degradation involved partial periodate oxidation. When alginate is oxidized by reacting with sodium periodate, the carbon–carbon bond of *cis*-diol group in the uronate residue is cleaved. This approach offers control over the degradation rate by varying the degree of oxidation, as increasing the degree of oxidation can accelerate the rate of degradation. However, the biocompatibility of alginate is likely to decrease at high degree of oxidation, due to the presence of aldehyde groups on the sugar residues [13].

In this study, we investigated whether alginate hydrogel degradation could be controlled by combining partial oxidation of polymer chains prior to hydrogel formation. Molecular weight and weight loss as a function of degradation time were evaluated. The interior morphology of OSA hydrogels was also observed. Our study provides a novel way to control the degradation of alginate hydrogels crosslinked by Ca^{2+} for biomedical application.

2. Experimental

2.1. Materials

Sodium alginate (the viscosity of 2% solution is 3200 mPa s at 25 °C) was obtained from Qingdao Haiyang Chemical Co. (China). $NaIO_4$ was purchased from Shanghai Sanpu Chemical Factory (China). D-Glucono-δ-lactone (GDL) was obtained from Jiangxi Xinghuanghai Medicine Food Chemical Co. (China). Tris-(hydroxymethyl) aminomethane (Tris) was purchased from Sinopharm Co. (China). All of these were used without further purification. The other reagents were A.P. grade and used without further purification.

* Corresponding author. Tel.: +86 931 8912387; fax: +86 931 8912582.
E-mail address: mzliu@lzu.edu.cn (M. Liu).

0141-3910/$ – see front matter © 2009 Elsevier Ltd. All rights reserved.
doi:10.1016/j.polymdegradstab.2009.05.011

2.2. Preparation of oxidized sodium alginate

Oxidized sodium alginate was prepared according to a previously reported method [11]. Sodium alginate was oxidized with sodium periodate at room temperature. The ratios between guluronate unit and periodate were 100:10, 100:30, and 100:50. An equimolar amount of ethylene glycol was added after 6 h to stop the oxidation. The resultant solution was filtered, washed with ethanol/water (1:1, v/v) and dried under vacuum at room temperature. The degree of oxidation (DO, %) of OSA was defined as the number of oxidized guluronate residues per 100 guluronate units, and determined by the method described by Wu et al. [14].

2.3. Preparation of OSA hydrogels

OSA was dissolved in distilled water at a certain concentration. Calcium carbonate ($CaCO_3$) in combination with GDL was used as a source of calcium ions to initiate the gelation. A $CaCO_3$ to GDL molar ratio of 0.5 was always maintained to achieve a neutral pH value [15]. For all OSA hydrogels, a basic calcium ion to carboxyl molar ratio of 0.18 was designated as 1X. A given amount of $CaCO_3$ was added to oxidized sodium alginate, mixed and vortexed for 1 min. The GDL was then added to the suspension and vortexed for 1 min to initiate gelation. The hydrogel was prepared in culture dish (60 mm in diameter) at 0 °C for 48 h. After the gelation, the hydrogel was cut into discs (14 mm diameter and 4 mm thickness). The hydrogel samples were dried at room temperature, and were further dried to constant weight under vacuum at 25 °C. The feed composition of all hydrogels was listed in Table 1.

2.4. Morphology observation

The interior morphology of OSA and SA hydrogels was examined using scanning electron microscopy (JSM-5600LV SEM, Japan) at an accelerating voltage of 20 kV.

2.5. Swelling kinetics of OSA hydrogels

The dried gels were immersed into the distilled water at 37 °C. The weight of the swollen samples was measured after the excess surface solution removed by filter paper. The swelling ratio (SR) was calculated by the following expression:

$$\mathrm{SR} = \frac{W_t - W_0}{W_0}. \quad (1)$$

Here W_t and W_0 are the weights of the swollen and dried samples, respectively.

The crosslinking density (ν_e, mol/cm^3) of OSA hydrogel was subsequently calculated from the Flory–Rehner equation [11,16]:

$$\nu_e = -\left[\ln(1-\nu_2) + \nu_2 + \chi_1\nu_2^2\right]\left[V_1\left(\nu_2^{1/3} - 2\nu_2/f\right)\right]^{-1} \quad (2)$$

Here χ_1 is the interaction parameter, f is the crosslinking functionality, V_1 is the molar volume of water (18.062 cm^3/mol) and ν_2 is the volume fraction of polymer in the hydrogel when its reaches the equilibrium swelling state. The interaction parameter, χ_1 was assumed to be 0.35 as it has been previously reported for similar interaction [16], and f to be 2. The value of ν_2 could be measured by following equation:

$$\nu_2 = \left(1/\rho_p\right)\left[(Q_m/\rho_s) + \left(1/\rho_p\right)\right] \quad (3)$$

Here ρ_p is the polymer density (0.8755 g/cm^3), ρ_s is the density of water (0.9933 g/cm^3 at 37 °C) and Q_m is the swelling ratio [16].

Table 1
Composition of OSA hydrogels.

Sample	Concentration (w/v)	Volume (mL)	$CaCO_3$/COO$^-$ (mol/mol)	ν_e (mol/cm^3)
SA	1.0%	20	1.5×	8.58×10^{-6}
10% OSA	1.5%	20	1.5×	4.67×10^{-5}
30% OSA	3.5%	20	1×	3.47×10^{-5}
50% OSA	9.0%	20	2×	2.68×10^{-3}

2.6. Degradation kinetics of OSA

Aqueous solutions of 0.2% (w/v) sodium alginate and OSA with PBS 7.4 were prepared and then placed in a thermostatic bath at 37 °C. At appropriate intervals, the viscosity of the solution was measured by Ubbelohde viscometer. The degradation of OSA was calculated by the following expression:

$$\text{Degradation ratio} = \frac{M_t}{M_0} \quad (4)$$

Here M_t and M_0 are the viscosity-average molecular weights at time t and time 0, respectively. Viscosity-average molecular weight was calculated by reported method [17].

2.7. Degradation kinetics of OSA hydrogels

The degradation of OSA hydrogels was performed in a conical flask filled with 50 ml PBS 7.4 or Tris–HCl 7.4. The degradation experiments were conducted by incubating the hydrogels in buffer placed in a thermostatic bath and by the determination of the weight loss after recovery of the samples at predetermined time intervals. After a predetermined time, the samples were removed from the solution, washed thoroughly with distilled water, and then dried at room temperature. The degradation was assessed by measuring the weight loss (%), which was defined as the following expression:

$$\text{Weight loss}\ (\%) = \frac{W_1 - W_2}{W_1} \times 100 \quad (5)$$

Here W_1 and W_2 are the weights of the gel before and after degradation, respectively.

2.8. DSC analysis

The glass transition temperature (T_g) of OSA hydrogel was measured on a Sapphire DSC (Perkin–Elmer Corp., Wilton, CT) at a scan rate of 15 °C/min under a dry nitrogen atmosphere. The weight of the samples ranged within 6–10 mg.

3. Results and discussion

3.1. Characterization of OSA

Periodate oxidation specifically cleaves the vicinal glycols in polysaccharides to form their dialdehyde derivatives. Each *cis*-diol group consumes one molecule of periodate. The ratio of sodium periodate to the number of repetitive units of sodium alginate was varied to obtain different degrees of oxidation. The degree of oxidation and molecular weight are dependent on the amount of sodium periodate, as expected (Table 2). With the increase in the amount of sodium periodate, the degree of oxidation increases but molecular weight decreases. The molecular weight shows significant depolymerization of sodium alginate. It is well known that the oxidation by periodate leads to a depolymerization of the chain,

Table 2
Characterization of oxidized sodium alginates.

Sample	Guluronate unit/periodate (mol/mol)	Degree of oxidation (%)	$M \times 10^{-5}$
SA	–	–	4.40
10% OSA	100:10	9.60	2.20
30% OSA	100:30	28.05	1.29
50% OSA	100:50	47.88	0.78

even when the oxidation is carried out in the dark [18]. The solubility of OSA is found to be increasing with the increase in degree of oxidation due to the increase of the chain flexibility caused by the depolymerization.

3.2. Morphology observation

Fig. 1 shows the SEM images of SA and OSA hydrogels. SA hydrogel demonstrates laminated structure, while 10% OSA and 30% OSA hydrogels show similar structure. However, 50% OSA hydrogel shows a different structure from SA, 10% OSA and 30% OSA hydrogels. In the first place, the distribution of laminated structure is homogeneous in SA hydrogel compared to OSA hydrogels due to the singleness of molecular structure unit. Because of oxidization of periodate, the singleness of molecular structure is destroyed. Therefore, the microscopic structure of OSA hydrogels becomes irregular. In the next place, the microscopic structure of 10% OSA, 30% OSA and 50% OSA hydrogels also was obviously different from each other. The degree of oxidation has certain influence on the microscopic structure, but the crosslinking density has the tremendous influence on the microscopic structure. Zhang et al. [19] also observed the interior morphology of PNIPAAm hydrogels by SEM. They found that the porous network structures of the PNIPAAm hydrogels were quite different from one another, depending on the level of crosslinking. The order of crosslink density is 30% OSA hydrogel $<$ 10% OSA hydrogel $<$ 50% OSA hydrogel, so the singleness of the hydrogel microscopic structure is in the following order: 30% OSA hydrogel $>$ 10% OSA hydrogel $>$ 50% OSA hydrogel. The swelling kinetics of OSA hydrogels might be affected by these microscopic structures.

3.3. Swelling kinetics of OSA hydrogels

Fig. 2 shows the swelling kinetics of OSA hydrogels in distilled water at 37 °C. The solubility of OSA is found to be increasing with increase in degree of oxidation, so the concentrations were different for preparing OSA hydrogels (Table 1). As expected, a decrease in swelling ratio is seen with an increase in the degree of oxidization (expect 30% OSA hydrogel). As far as we know, the swelling ratio is dependent on the crosslinking density. The higher the crosslinking density, the lower the swelling ratio of hydrogel [20,21]. From Table 1 it can be seen that the crosslinking density of 30% OSA hydrogel is lower than that of 10% OSA hydrogel, so the swelling ratio of 30% OSA hydrogel is higher than that of 10% OSA hydrogel. In Table 1, the concentration of OSA and the molar ratio of $CaCO_3$ to COO^- are determined through the experiment, under this condition the equilibrium of swelling ratio is the biggest at 25 °C (data not shown).

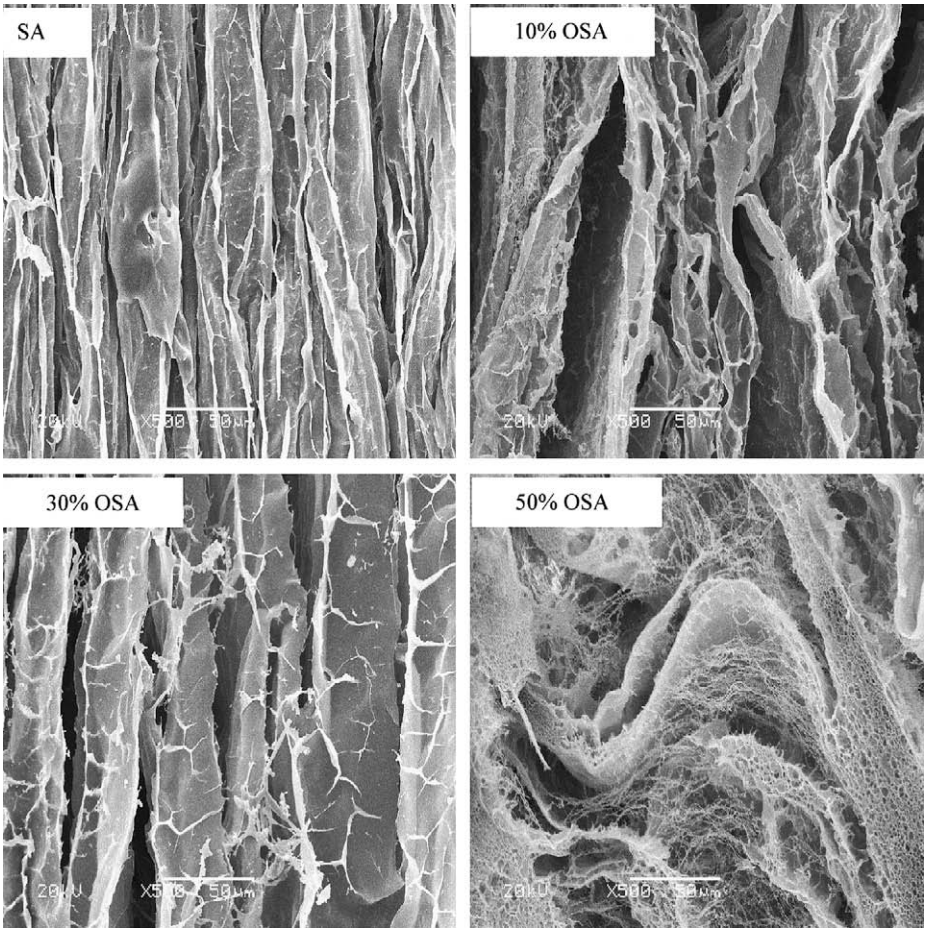

Fig. 1. Scanning electron microscope micrographs of hydrogels.

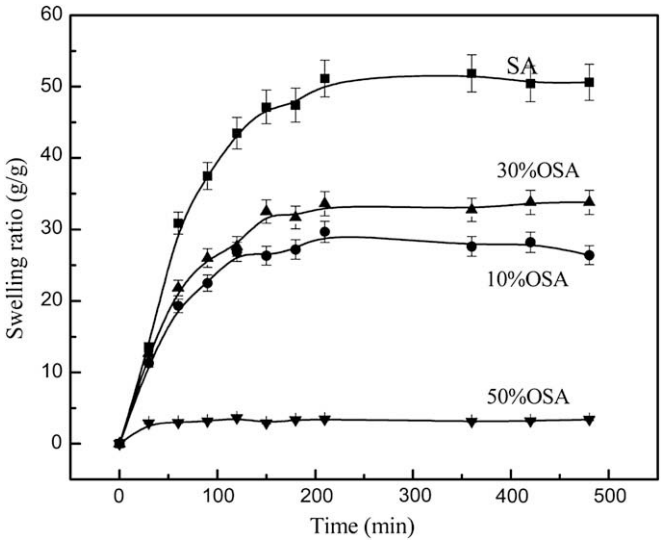

Fig. 2. Swelling kinetics of OSA hydrogels in distilled water at 37 °C.

3.4. Degradation kinetics of OSA

Fig. 3 shows the degradation kinetics of OSA in PBS 7.4 at 37 °C. The percentages of degradation of SA, 10% OSA, 30% OSA and 50% OSA are respectively 5.00, 26.53, 43.80 and 67.31% in 120 h. When alginate is oxidized with sodium periodate, the carbon–carbon bond of the *cis*-diol group in the uronate residue is cleaved, and the aldehyde groups of oxidized hexuronic-acid residues spontaneously form six-membered hemiacetal rings with the closest hydroxyl groups on the two adjacent unoxidized sugar residues in the chains. This alters the conformation of urinate residues to an open-chain adduct and infers a free rotation about the three bonds adjoining C-4, C-5, the original ring-oxygen atom, and C-1 of the oxidized hexuronic-acid residues. This creates hydrolytically labile bonds in the polysaccharide [13]. The number of labile bonds increases by increasing the degree of oxidation, so the rate of degradation increases with the increase in degree of oxidation.

3.5. Degradation kinetics of OSA hydrogels

The degradability of OSA hydrogels was studied by examining the weight loss and swelling ratio of gels with time in PBS and Tris–HCl at 37 °C, respectively. Fig. 4(a) shows a typical weight loss curve for a degrading OSA hydrogel. When Ca^{2+} crosslinked OSA hydrogels are placed in PBS 7.4, the ion-exchange process between the Ca^{2+} ions presenting in the "egg-box" cavity of polyguluronate blocks and Na^{+} ions of buffer solution is mainly responsible for the swelling/degradation [22]. However, Boontheekul et al. [13] reported that hydrolytic scission of the polymer chains at oxidized sugar residues controlled degradation, not the dissociation of calcium crosslinks. So the higher the degree of oxidation, the more the oxidized sugar residues and the higher the rate of degradation is. From Fig. 4(a), it can be seen that the networks decrease in weight through the degradation. Moreover, there is good correlation between weight loss and the degree of oxidation. The weight loss of SA, 10% OSA, 30% OSA and 50% OSA are respectively 68.90, 73.00, 80.27 and 88.89% in 180 min.

Fig. 5(a) exhibits the degradation behavior as a function of time for hydrogels in Tris–HCl. The hydrogels show some increase in the weight loss as a function of time. As degradation occurs, the hydrolytically labile bonds in OSA are cleaved throughout the entire hydrogel at a rate controlled by the reaction kinetics for their hydrolysis. This ongoing cleavage of labile bonds within the hydrogel systematically decreases the crosslinking density of the

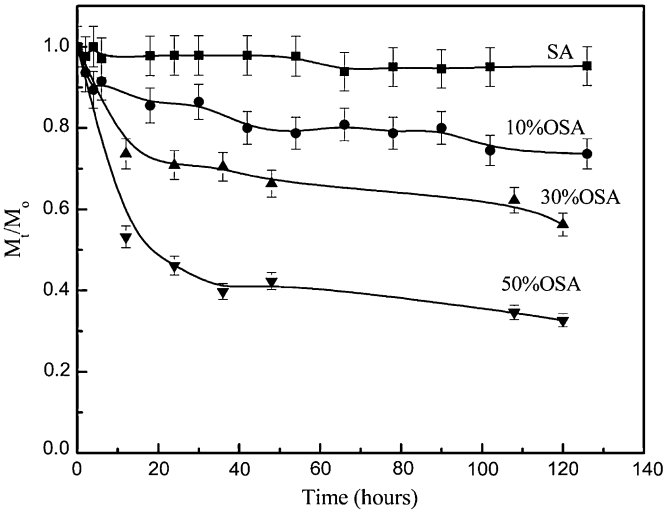

Fig. 3. Degradation kinetics of OSA in PBS 7.4 at 37 °C.

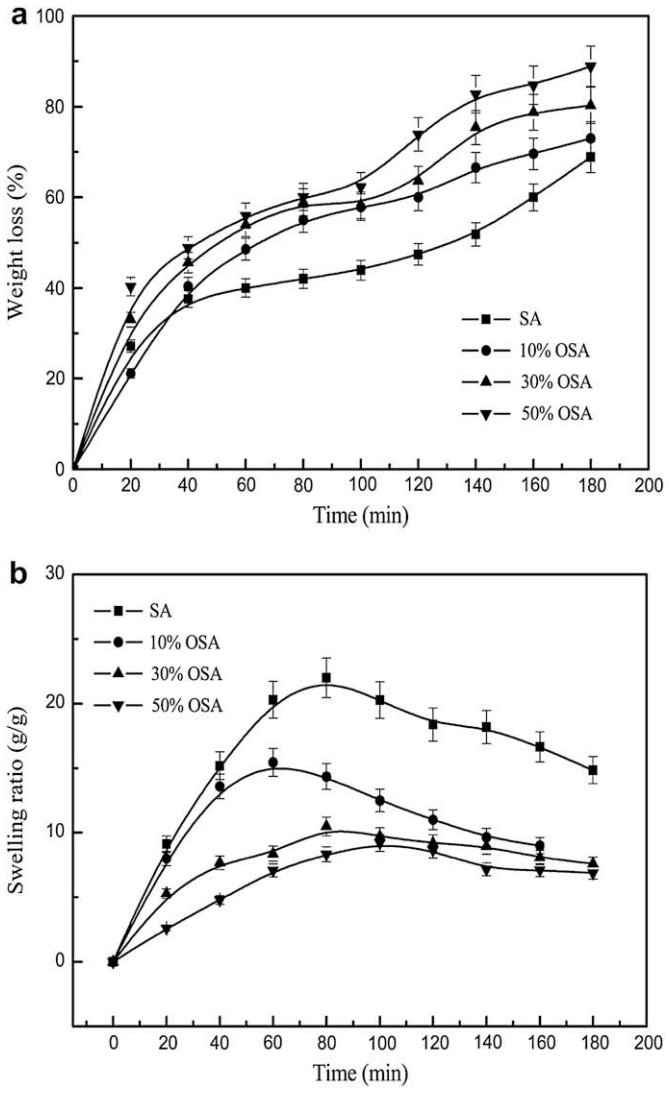

Fig. 4. Degradation kinetics of OSA hydrogels in PBS 7.4 at 37 °C.

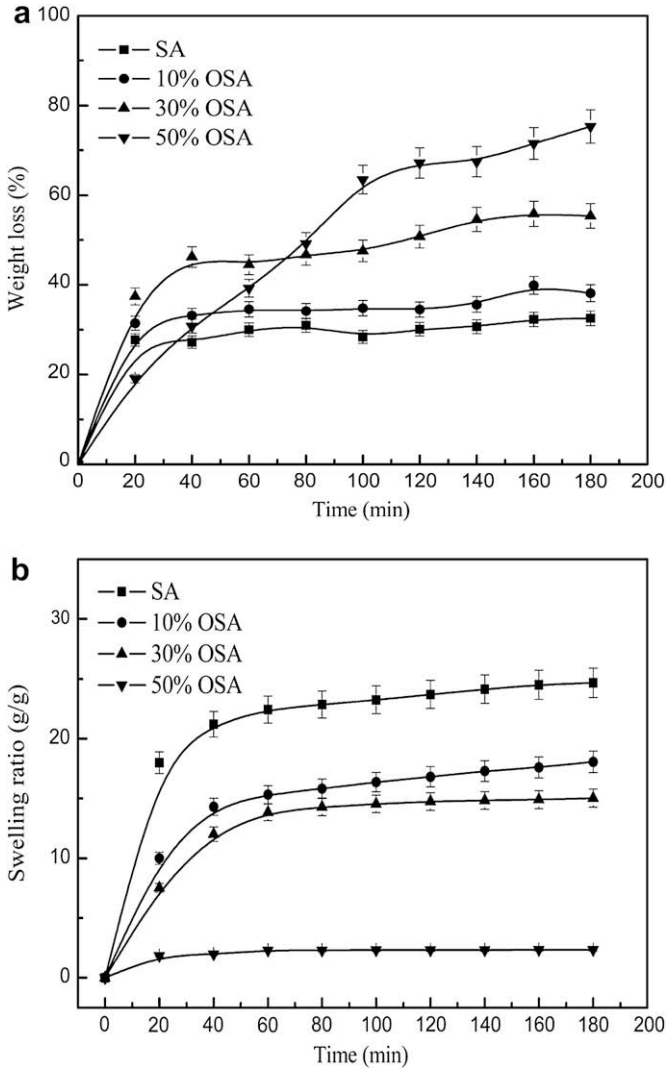

Fig. 5. Degradation kinetics of OSA hydrogels in Tris–HCl 7.4 at 37 °C.

overall network. The number of hydrolytically labile bond increases by increasing the degree of oxidization, so the weight loss increases with the increase in degree of oxidization. However, the weight loss of 50% OSA hydrogel is lower than SA hydrogel in the first 40 min, and this phenomenon has not appeared in PBS 7.4. OSA hydrogels can degrade in Tris–HCl mainly due to the hydrolysis, which is decided by the diffusion rate of water. Swelling ratio of 50% OSA hydrogel is very lower than other hydrogels because of the highest crosslinking density (Fig. 5(b)). Thus, the degradation of 50% OSA hydrogel is slower than other hydrogels. At the same time, 50% OSA hydrogel has the large number of hydrolytically labile bonds, which urges the hydrogel to degrade quickly. The result of the both interactions is that 50% OSA hydrogel has a quicker degradation when the water diffuses into the hydrogel after a period of time. In PBS 7.4, there simultaneously exist hydrolysis and ion-exchange, and the difference of swelling ratio among these hydrogels is not very big (Fig. 4(b)). Therefore, the water diffusion is not the restriction factor of OSA hydrogels degeneration all the time. The hydrolytically labile bonds are more and the rate of degradation is quicker in PBS 7.4.

The changes in the swelling ratio of OSA hydrogels are determined to more fully characterize the degradation of these hydrogels (Figs. 4(b) and 5(b)). In PBS, the trend of swelling ratio increases fleetly at first and then decreases. But in Tris–HCl, the swelling ratio increases slowly all the time. The swelling ratio is strongly related to buffer composition. During the initial stage of degradation in PBS, a small number of ion-exchange between Ca^{2+} and Na^{+} cannot damage the whole hydrogel network, but the lattice size of the networks would enlarge. As a result, the swelling ratio increases. When the ion-exchange reaches a critical value, the whole crosslinking network would be disjointed, resulting in disappearance of the hydrogel. However, the increase of swelling ratio in Tris–HCl is the result of partial degradation, which endows the hydrogel with the absorption of a greater amount of water.

DSC measurements for 30% OSA gel residues were conducted on samples after different degradation times (Fig. 6). The broad endothermic peak around 150 °C in the DSC thermograms can be attributable to the glass transition of 30% OSA hydrogel. It can be seen that, with the extension of the time, the T_g of 30% OSA hydrogel in PBS or Tris–HCl decreases and the endothermic peak becomes wider. This result also suggests that the network of hydrogel becomes weak when degradation occurs, which is agreeing with the result of weight loss.

3.6. Mechanism of degradation

Metters [23] reported that there are two types of degradation processes of hydrogel networks: surface erosion and bulk erosion.

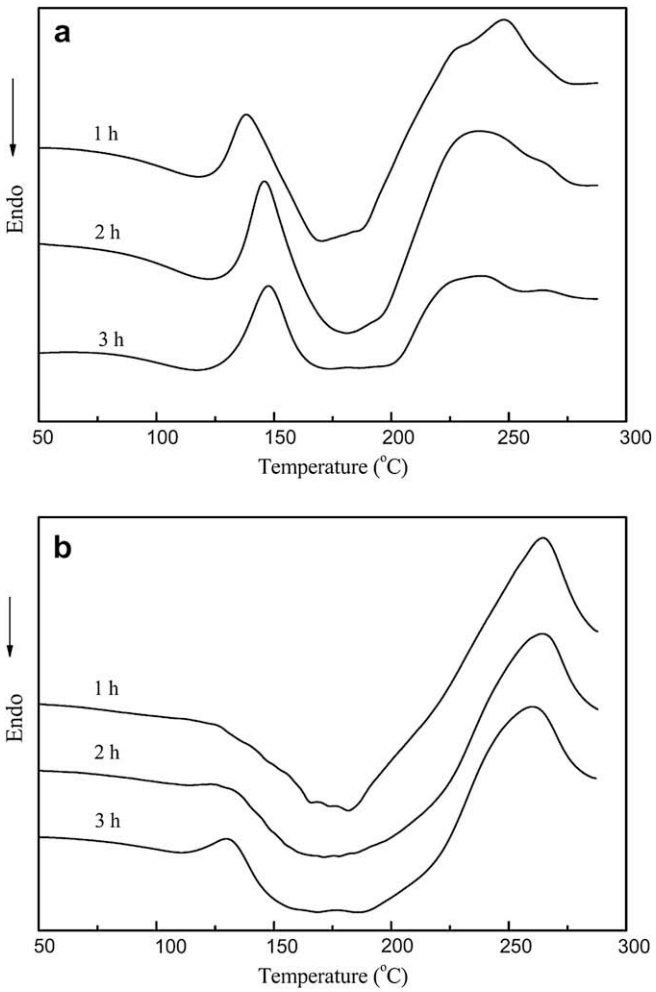

Fig. 6. DSC thermograms of 30% OSA hydrogel degrade in (a) PBS 7.4 and (b) Tris–HCl 7.4.

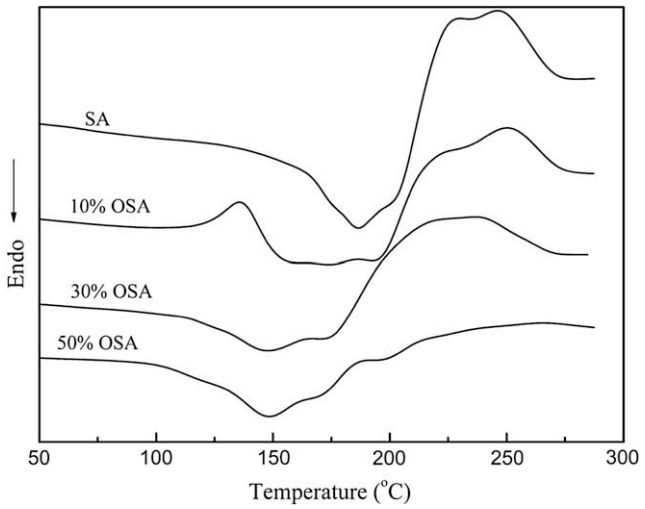

Fig. 7. DSC thermograms of OSA hydrogels with different degrees of oxidation.

When the rate of water diffusion into a sample is slower than the hydrolysis reaction, the water will be adsorbed on the surface by before it can diffuse into the bulk of the sample. This kind is called surface erosion. Bulk erosion, on the other hand, occurs when the rate of water diffusion into the sample is much faster than the hydrolysis reaction. Figs. 4(b) and 5(b) show that hydrogels in PBS and Tris–HCl both have biggish swelling ratios and the rate of water diffusion into a sample is faster than the degradation process, these facts suggest that the degradation of OSA hydrogels in aqueous solutions belongs to the bulk-erosion process.

It has been generally considered that the degradation behavior of the hydrogel depends on the crosslinking density [24]. However, the results of present study suggest that the degradation of OSA hydrogel depends on the degree of oxidation, instead of crosslinking density. As with all hydrogels, the physical and mechanical behaviors of the gel are highly dependent on the backbone chemistry of the polymer. The scission of the main chain of alginate ruptures as oxidation occurs, so the molecular weight decreases. At the same time, the quantity of G-units increases [25]. Russo has reported that T_g can decrease when increasing the quantity of G-units [26]. Fig. 7 shows the DSC thermograms of OSA hydrogels with different degrees of oxidation. The T_g of OSA hydrogel decreases by increasing the degree of oxidation due to the increase in the quantity of G-units. Although 50% OSA hydrogel has the highest degree of oxidation, the T_g is the lowest. These results indicate that the degree of oxidation is the uppermost factor of the degradation of OSA hydrogel. All the results show that the effect of degree of oxidation on the degradation is far greater than the effect of crosslinking density.

4. Conclusions

The degradation of OSA hydrogels crosslinked by Ca^{2+} relied on the degree of oxidization of OSA. The weight loss increased with increase in degradation time and the degradation rate of the hydrogel with high degree of oxidation was faster than that of the hydrogel with lower degree of oxidation. This type of controllable degradation, independent of the degree of oxidation, may have significant advantages for biomedical applications of hydrogels.

Acknowledgement

The financial support of Gansu Province Project of Science and Technologies (contract grant number: 0804WCGA130) is gratefully acknowledged.

References

[1] Bryant SJ, Anseth KS. The effects of scaffold thickness on tissue engineered cartilage in photocrosslinked poly(ethylene oxide) hydrogels. Biomaterials 2000;22:619–26.
[2] Maris B, Verheyden L, Van Reeth K, Samyn C, Augustijins P, Kinjet R, et al. Synthesis and characterisation of inulin-azo hydrogels designed for colon targeting. Int J Pharm 2001;213:143–52.
[3] Soppimath KS, Kulkarni AR, Aminabhavi TM. Chemically modified polyacrylamide-*g*-guar gum-based crosslinked anionic microgels as pH-sensitive drug delivery systems: preparation and characterization. J Control Release 2001;75:331–45.
[4] Lloyd AW, Faragher RGA, Denyer SP. Ocular biomaterials and implants. Biomaterials 2001;22:769–85.
[5] Razzak MT, Darwis D, Sukirno Z. Irradiation of polyvinyl alcohol and polyvinyl pyrrolidone blended hydrogel for wound dressing. Radiat Phys Chem 2001;62:107–13.
[6] Tilakaratne HK, Hunter SK, Andracki ME, Benda JA, Rodgers VGJ. Characterizing short-term release and neovascularization potential of multi-protein growth supplement delivered via alginate hollow fiber devices. Biomaterials 2007;28:89–98.
[7] Xiao CM, Zhou GY. Synthesis and properties of degradable poly(vinyl alcohol) hydrogel. Polym Degrad Stabil 2003;81:297–301.
[8] Kemp MR, Fryer PJ. Enhancement of diffusion through foods using alternating electric fields. Innov Food Sci Emerg 2007;8:143–53.
[9] Li T, Shi XW, Du YM, Tang YF. Quaternized chitosan/alginate nanoparticles for protein delivery. J Biomed Mater Res A 2007;83:383–90.
[10] Prang P, Müller P, Eljaouhari A, Heckmann K, Kunz W, Weber T, et al. The promotion of oriented axonal regrowth in the injured spinal cord by alginate-based anisotropic capillary hydrogels. Biomaterials 2006;27:3560–9.
[11] Balakrishnan B, Jayakrishnan A. Self-cross-linking biopolymers as injectable in situ forming biodegradable scaffolds. Biomaterials 2005;26:3941–51.
[12] Bouhadir KH, Kruger GM, Lee KY, Mooney DJ. Sustained and controlled release of daunomycin from cross-linked poly(aldehyde guluronate) hydrogels. J Pharm Sci 2000;89:910–9.
[13] Boontheekul T, Kong HJ, Mooney DJ. Controlling alginate gel degradation utilizing partial oxidation and bimodal molecular weight distribution. Biomaterials 2005;26:2455–65.
[14] Wu NQ, Pan CY, Zhang BJ, Rao YP, Yu D. Preparation and properties of a thermo-sensitive hydrogel based on oxidized sodium alginate. Acta Polym Sin 2007;6:497–502.
[15] Kuo CK, Ma PX. Ionically crosslinked alginate hydrogels as scaffolds for tissue engineering: part 1. Structure, gelation rate and mechanical properties. Biomaterials 2001;22:511–21.
[16] Lee KY, Bouhadir KH, Mooney DJ. Degradation behavior of covalently cross-linked poly(aldehyde guluronate) hydrogels. Macromolecules 2000;33:97–101.
[17] Smidahod O, Haug A. A light scattering study of alginate. Acta Chem Scand 1968;22:797–810.
[18] Laurienzo P, Malinconico M, Motta A, Vicinanza A. Synthesis and characterization of a novel alginate-poly(ethylene glycol) graft copolymer. Carbohyd Polym 2005;62:274–82.
[19] Zhang XZ, Wu DQ, Chu CC. Effect of the crosslinking level on the properties of temperature-sensitive poly(*N*-isopropylacrylamide) hydrogels. J Polym Sci Part B: Polym Phys 2003;41:582–93.
[20] Chen J, Liu MZ, Liu HL, Ma LW. Synthesis, swelling and drug release behavior of poly(*N*,*N*-diethylacrylamideco-*N*-hydroxymethyl acrylamide) hydrogel. Mater Sci Eng C 2009;. doi:10.1016/j.msec.2009.04.008.
[21] Treloar LRG. Physics of rubber elasticity. Oxford: Clarendon Press; 1975.
[22] Bajpai SK, Sharma S. Investigation of swelling/degradation behaviour of alginate beads crosslinked with Ca^{2+} and Ba^{2+} ions. React Funct Polym 2004;59:129–40.
[23] Metters AT, Bowman CN, Anseth KS. A statistical kinetic model for the bulk degradation of PLA-*b*-PEG-*b*-PLA hydrogel networks. J Phys Chem B 2000;104:7043–9.
[24] Mason MN, Metters AT, Bowman CN, Anseth KS. Predicting controlled-release behavior of degradable PLA-*b*-PEG-*b*-PLA hydrogels. Macromolecules 2001;34:4630–5.
[25] He SL, Zhang M, Geng ZJ, Yin YJ, Yao KD. Preparation and characterization of partially oxidized sodium alginate. Chin J Appl Chem 2005;22:1007–11.
[26] Russo R, Malinconico M, Santagata G. Effect of cross-linking with calcium ions on the physical properties of alginate films. Biomacromolecules 2007;8:3193–7.